

Experiments on the Direct Photonuclear Effect*

SVEN A. E. JOHANSSON †

Institute for Atomic Research and Physics Department, Iowa State College, Ames, Iowa

(Received June 23, 1954)

An investigation has been made of the high-energy protons and neutrons emitted in irradiation with bremsstrahlung of 65-Mev maximum energy. Protons above 14 Mev were measured. The energy limit for the neutrons varied. The angular distributions of protons from carbon, aluminum, nickel, and molybdenum could be fitted with curves of the form $a + (\sin\theta + b \sin\theta \cos\theta)^2$ with the maximum around 60° . The angular distributions of neutrons above 5 and 10 Mev could be fitted with curves of the form $a + b \sin^2\theta$. The yield of protons for eight elements from carbon to molybdenum was approximately proportional to Z . The yield of neutrons above 7.5 Mev for 19 elements from carbon to lead was approximately proportional to N . Excitation curves were measured for the high-energy protons from aluminum and phosphorus. They have a threshold at about 25 Mev and rise to about 45 Mev. From there on they are nearly constant. An attempt was made to detect proton-neutron coincidences from a carbon target. No true coincidences were found. It is concluded that the measurements are in good agreement with an independent particle model but that they agree only partly with a deuteron model.

INTRODUCTION

IT is well known that the emission of protons and neutrons in photonuclear reactions can be accounted for fairly well by an evaporation model. The nucleus is heated by the absorption of a photon and is de-excited by the evaporation of one or several particles according to the statistical theory.¹ Recent experiments²⁻⁸ on the emission of photoprotons at low and medium x-ray energies have shown, however, that in addition to this process there exists a type of direct photoemission. The energy spectrum of the photoprotons shows an excess of high-energy protons compared to the spectrum expected from the statistical theory. There is also a departure from spherical symmetry in angular distribution. This process is relatively most important for medium and heavy elements where it gives an anomalously high ratio between the cross sections for (γ, p) and (γ, n) processes.⁹ Work¹⁰⁻¹⁵ with very high-energy x-rays at 200-300 Mev has shown the presence of high-energy protons emitted in a strongly forward direction. Very little is known about the emission of high-energy photoneutrons. Measurements¹⁶⁻¹⁷ made with threshold detectors indicate an excess of neutrons at right angles to the beam.

To account for these effects Courant¹⁸ and Jensen¹⁹ have proposed a direct photonuclear effect. It is suggested that the photon is absorbed by only a small part of the nucleus, perhaps only a single nucleon. A proton or neutron may then be emitted without sharing its energy with the rest of the nucleus. There is therefore no statistical distribution of the excitation energy and the proton emission is much higher than expected from the statistical theory. In heavy elements, where the barrier greatly reduces the number of evaporation protons, this process might account for almost all of the emitted protons.

Levinger²⁰ has proposed another model for the high-energy photoeffect. He considers the photodisintegration of a quasi deuteron moving inside the nucleus. According to this model the high-energy protons and neutrons are emitted in pairs. The angular distribution of the particles is essentially the same as for the photodisintegration of the deuteron.

Comparing theory and experiment one encounters several difficulties. The experiments have been performed at different energies. The direct photoeffect is mixed with various other processes, different for different energies. With bremsstrahlung of 20-25 Mev maximum energy it is difficult to separate the directly emitted particles from the evaporation particles. With high-energy bremsstrahlung one might expect mesonic effects to play an important role, making the particle emission a fairly complicated process. Another difficulty is that most experiments deal with photoprotons; very little is known about the directly emitted photoneutrons.

The present work has been done using bremsstrahlung of 65-Mev maximum energy from the Iowa State College synchrotron. At this energy it is easy to separate the directly emitted particles from the statistically evaporated ones, yet the energy is sufficiently low so that

* Work performed in the Ames Laboratory of the U. S. Atomic Energy Commission.

† On leave from the University of Lund, Lund, Sweden.

¹ V. F. Weiskopf and D. H. Ewing, Phys. Rev. **57**, 472 (1940).

² Curtis, Hornbostel, Lee, and Salant, Phys. Rev. **77**, 290 (1950).

³ B. C. Diven and G. M. Almy, Phys. Rev. **80**, 407 (1950).

⁴ Mann, Halpern, and Rothman, Phys. Rev. **87**, 146 (1952).

⁵ H. Hendel, Z. Physik **135**, 168 (1953).

⁶ W. A. Butler and G. M. Almy, Phys. Rev. **91**, 58 (1953).

⁷ M. E. Toms and W. E. Stephens, Phys. Rev. **92**, 362 (1953).

⁸ M. M. Hoffman and A. G. W. Cameron, Phys. Rev. **92**, 1184 (1953).

⁹ O. Hirzel and H. Wäffler, Helv. Phys. Acta **20**, 373 (1947).

¹⁰ D. Walker, Phys. Rev. **81**, 643 (1951).

¹¹ C. Levinthal and A. Silverman, Phys. Rev. **82**, 822 (1951).

¹² J. C. Keck, Phys. Rev. **85**, 410 (1952).

¹³ S. Kikuchi, Phys. Rev. **86**, 41 (1952).

¹⁴ J. W. Rosengren and J. M. Dudley, Phys. Rev. **89**, 603 (1953).

¹⁵ J. W. Weil and B. D. McDaniel, Phys. Rev. **92**, 391 (1953).

¹⁶ H. L. Poss, Phys. Rev. **79**, 539 (1950).

¹⁷ Demos, Fox, Halpern, and Koch, Phys. Rev. **86**, 605 (1952).

¹⁸ E. D. Courant, Phys. Rev. **82**, 703 (1951).

¹⁹ P. Jenson, Naturwiss. **35**, 190 (1948).

²⁰ J. S. Levinger, Phys. Rev. **84**, 43 (1951).

mesonic effects cannot occur. The aim of this work was to collect as much experimental information as possible about the high energy photoprotons and photoneutrons. The angular distribution has been measured both for protons and neutrons for various elements. The yield of high-energy protons and neutrons has been measured for different elements. Excitation curves for protons above a certain energy have been determined. Finally an experiment has been carried out in order to determine whether or not the protons and neutrons are emitted in coincidence.

EXPERIMENTAL PROCEDURE

General Description

The experimental arrangement for the measurements on protons is shown in Fig. 1. The bremsstrahlung beam was collimated with lead. The diameter of the beam was 3 cm at the position of the target. The photomultiplier detector could be rotated and be put in different angular positions with respect to the target. The target was similarly rotated, so that the effective thickness was always constant. Hence the energy loss of the protons in the target was independent of the counter position. When the apparatus is rotated, the dose received by the target changes because of the fact that the intensity decreases towards the edges of the beam. A correction has been applied for this effect; it is fairly small, however.

Essentially the same arrangement was used for the neutron measurements. The target was in this case a block of the material to be investigated. It remained in a fixed position while the counter was rotated. In both the proton and neutron experiments the counter was shielded from scattered radiation by a large pile of lead bricks.

The beam intensity was monitored by an ionization chamber placed to the side of the beam. No absolute determination of the dose was required but it was necessary to know the relative dose received by the target for a certain counting period. The machine proved so stable in operation that the most convenient way to arrange the experiments was to use a constant counting period and to keep the beam intensity constant by adjusting the machine to give a constant reading on the ionization chamber dosage ratemeter. The maximum deviations from the mean value on the meter were 1-2 percent. The variations of the mean values for different counting periods were less than 1 percent. The monitor readings were obtained on a recording instrument so that the constancy of the intensity could be checked and corrections applied. By activating foils of zinc and tantalum a further check on the constancy of the beam intensity was possible.

The counters will be described in greater detail in the following paragraphs. The pulses were taken out from cathode-followers and led through cables to the amplifiers in the control room. Care was taken to avoid any

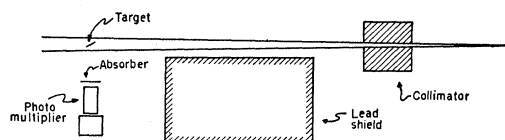


FIG. 1. Experimental arrangement for the proton measurements.

deformation of the pulses. They were analyzed by integral and single-channel discriminators and counted by conventional scalars. One of the major difficulties in these experiments was the piling up of the pulses. Although the mean counting rate was low, the counting rate during the time of a beam pulse was quite high. To keep the pile-up low, the pulses from the counters were made as short as possible. The necessity of reliable pulse height discrimination sets a lower limit for the pulse width. Another limiting factor is the time constant of the ZnS phosphor used in the counters. It is impossible to make the pulse length very much shorter than the time constant of the phosphor because this introduces great statistical fluctuations in the pulse height. A time constant of 0.75 μ sec was found to be a suitable value for the pulses.

Another way to diminish the pile-up is to make the beam pulse duration as long as possible. No special pulse stretching device was used but the electrons were allowed to strike the synchrotron target near the maximum of the magnetic field. This gave a pulse length of about 100 μ sec. Although this improved the situation, the pile-up was still a very serious limitation, especially in the proton experiments.

The Proton Counter

The proton counter consists of a thin, uniform layer of zinc sulfide on the top of a photomultiplier, type E.M.I. 6260. The grain size of the zinc sulfide (RCA 33Z-20-A) was reduced in the following way. The ZnS powder was suspended in absolute alcohol in a beaker and allowed to settle down partly. The part remaining in suspension was isolated rapidly from the rest by pouring the alcohol into another beaker, leaving the coarse grains on the bottom of the first beaker. This process was repeated several times. The fine-grained zinc sulfide obtained in this way was finally suspended in alcohol and allowed to settle completely down on the top of the multiplier. For this purpose a tube of plastic was tightly mounted on the top of the multiplier, to form a beaker for the suspension. Great care was taken to prevent convection currents in the liquid during the settling period. Finally most of the alcohol was taken away and the rest was allowed to evaporate. The resulting layer of zinc sulfide was very compact and durable. The thickness was 10 mg/cm². It was covered with a reflector of very thin aluminum foil. The photomultiplier was wrapped with black electrical tape and painted with Glyptal to make it light-tight.

In order to discriminate against the low-energy

evaporated protons, an aluminum absorber of thickness 274 mg/cm^2 was put in front of the counter. The distance from target to the zinc sulfide screen was 11 cm. The aluminum reflector was very thin (0.2 mg/cm^2). These values correspond to an energy cutoff for the counter of 14 Mev.²¹

Figure 2 shows the pulse height spectrum obtained from an aluminum target of thickness 274 mg/cm^2 . The steeply rising portion to the left is due to the piling up of pulses from the electron background. Fortunately the spectrum drops almost to zero before the proton pulses start to register. By setting an integral discriminator at a value slightly higher than the lowest point, one can completely discriminate against the electron pulses without losing more than a small fraction of the proton pulses.

It is possible to calculate the pulse height distribution if one knows the energy spectrum of the protons and the range-energy curve. The energy spectrum has been taken from the work of Hoffman and Cameron.⁸ They found for the high-energy protons a differential spectrum of the form kE^{-n} . For aluminum bombarded with 65-Mev bremsstrahlung, n has the value 7. It turns out, however, that the results of the calculation are rather insensitive to the value of n . The calculated pulse height distribution has been normalized to give the best possible fit to the experimental points. The line in Fig. 2 shows the calculated curve. The agreement is very good, indicating that the counter works properly. The pulse height distribution has been calculated only for the lower part. The large pulses correspond to low-energy protons, and the range-energy curve is not known with sufficient accuracy in that energy range. It is, however, easy to calculate the number of pulses above a certain pulse height. A comparison with the experimental value gives a satisfactory agreement.

It has been assumed in the foregoing that all the heavily ionizing particles are protons. However, one might expect some deuterons. The absorption in the absorber and the air corresponds to a cut-off energy of 19 Mev for deuterons. It seems likely that the number of deuterons above 19 Mev is much less than the number of

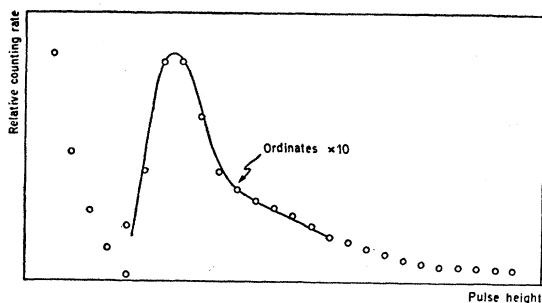


FIG. 2. Pulse-height distribution for the protons from an aluminum target.

²¹ Aron, Hoffman, and Williams, Range-energy curves, AECU-663.

protons above 14 Mev. An experimental indication against the presence of deuterons is the good agreement between the experimental and the calculated pulse height distributions. If there were an appreciable number of deuterons present, they should cause a deformation of the pulse height distribution.

It is interesting to calculate the energy distribution of the photoprotons being registered by the counter. We assume that the efficiency of the counter is 100 percent, although this is not exactly true since some of the smallest proton pulses may fall below the discrimination level. They would correspond to high-energy protons. However, only a small part is lost in this way and our assumption is therefore approximately true. The protons are assumed to be emitted with an energy distribution of the form kE^{-n} . By taking the target thickness into account, the curve *c* in Fig. 3 is obtained. A value of $n=7$ was used in this calculation.

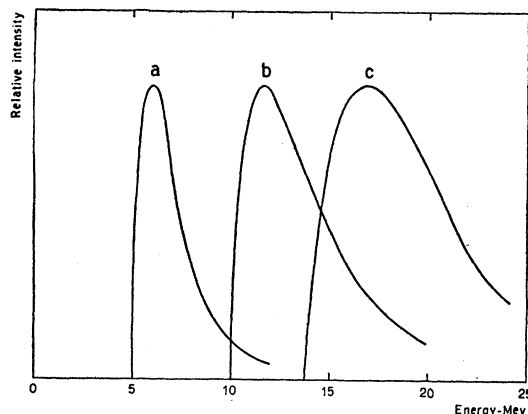


FIG. 3. Schematic energy distributions for the particles detected by the counters. Curves *a* and *b*: neutrons; curve *c*: protons.

The main features of the curve are the same for other reasonable values of n . The greater part of the protons registered by the counter falls in a fairly narrow energy range just above the threshold. Seventy-five percent of the protons have an energy between 14 and 21 Mev.

The Neutron Counter

The neutron scintillation counter is of a type devised by Hornyak.²² The phosphor, however, was made in a different way. It consists of a suspension of zinc sulfide (R.C.A. 33Z-20-A) in plastic. The following procedure was used: The zinc sulfide powder was suspended in liquid plastic and a hardening catalyst was added. The liquid was stirred until it was very viscous, in order to prevent a nonuniform distribution of the zinc sulfide, and was then allowed to cure completely. Finally the plastic piece was machined to a cylinder, 35 mm in diameter and 15 mm thick, and was mounted on the top of a photomultiplier, type E.M.I. 6260. Silicone oil

²² W. F. Hornyak, Rev. Sci. Instr. 23, 264 (1952).

was used to make optical contact. An aluminum reflector was mounted around the plastic phosphor, and the whole counter was wrapped with black electrical tape and painted with Glyptal to become light-tight.

The basic process in this counter is the scattering of neutrons in the hydrogen of the plastic. The recoil protons are detected by the zinc sulfide. It has been shown²³ that the zinc sulfide alone detects neutrons by an (n,p) reaction in sulphur. If we know the cross section²⁴ of the (n,p) reaction and the amount of zinc sulfide in the phosphor (10 percent) it can be shown that the zinc sulfide itself contributes with less than 1 percent to the total detection efficiency in the present case.

The great advantage with a counter of this type is the low sensitivity to gamma rays and electrons. The intensity of the scattered gamma rays and electrons is so high, however, that even a counter of this type becomes overloaded. Therefore a lead filter 5 cm thick was used in front of the counter.

Figure 4 shows the pulse height distribution for the neutrons from an aluminum target. The upper part of the curve is linear but the counting rate increases more rapidly for small pulse heights. Scattering and other secondary effects will, of course, give an excess of low-energy neutrons. However, one might ascribe the high counting rate of small pulses to the presence of the low-energy evaporation neutrons. The upper part of the curve could then be due to high-energy, directly emitted neutrons. The break in the curve comes at about 4 Mev which is in reasonable agreement with the interpretation given here.

In order to calibrate the counter a polonium-beryllium source was used. The energy distribution of the neutrons from such a source is well known.²⁵ The corresponding energy distribution for the protons was then calculated. It was assumed that the pulse height is proportional to the proton energy and that the resolution of the counter is fairly good. It is rather likely that both these assumptions are wrong because of the inhomogeneous character of the phosphor. However, the pulse height distribution calculated in this way agrees in shape fairly well with the one obtained experimentally with the Po-Be source. This fact makes it possible to find the end point of the pulse distribution by extrapolation to zero counting rate. The pulse height value so obtained corresponds to the energy value for the end point of the Po-Be neutron spectrum. There is, of course, a considerable uncertainty in this calibration. A conservative estimate of the error is ± 10 percent. Furthermore, only one calibration point is used. The calibration might be nonlinear, especially at low energies. However, for the purpose of this work it is not necessary to know exact energy values. It is sufficient to be able to discriminate against the low-energy evaporation neutrons.

²³ G. R. Keepin, Rev. Sci. Instr. **25**, 30 (1954).

²⁴ R. K. Adair, Revs. Modern Phys. **22**, 249 (1950).

²⁵ B. G. Whitmore and W. B. Baker, Phys. Rev. **78**, 799 (1950).

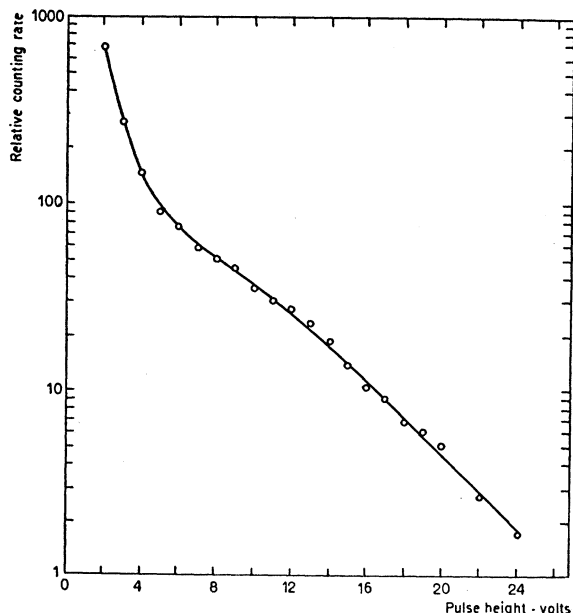


FIG. 4. Pulse-height distribution for the neutrons from an aluminum target.

An estimate can be made about the energy distribution of the neutrons detected by the counter for various discriminator settings. The primary energy distribution of the neutrons is assumed, in analogy with the proton case, to be of the form kE^{-n} . The value of n is not known. It has therefore been assumed tentatively that n has the same value for neutrons as for protons of the same energy. This gives a value of n of about 5. However, the exact form of the neutron spectrum is less important for this approximate calculation. It is sufficient to know that the number of neutrons falls off rapidly with the energy. The assumed energy spectrum has to be corrected for the absorption in the lead filter. Multiplication by the sensitivity of the counter as a function of the energy then gives the energy distribution of the counted neutrons. The curves *a* and *b* in Fig. 3 show the spectra for discriminator settings corresponding to thresholds at 5 and 10 Mev, respectively. It can be seen that the main part of the neutrons fall in a fairly narrow range just above the threshold.

The curves *a* and *b* in Fig. 3 have a sharp lower limit corresponding to a well-defined threshold for the counter. However, this requires a perfect phosphor with very high energy resolution. Actually the counter has a poor resolution. Recoil protons of a certain energy give pulses with a wide variation in pulse height. Some of them may be considerably higher than the mean value. Therefore, neutrons with an energy below the threshold value have a certain chance to be counted. It means that the sensitivity curve of the counter has a tail at the low-energy side. The importance of this fact will be discussed later.

RESULTS

Angular Distribution

Protons

The main difficulty in this experiment was the piling up of pulses in the counter, because of scattered gamma rays and electrons. It could be kept sufficiently low by lowering the beam intensity. The requirement of a reasonable number of counts sets a lower limit for the intensity. The synchrotron was operated fairly close to this limit in order that the measurements could not be affected by the pile-up. It was regarded better to have somewhat greater statistical errors than to run the risk of introducing systematic errors. Before each run a pulse distribution like the one shown in Fig. 2 was recorded to check the complete separation of the protons from the electron background. To get a further check the pulses were displayed on an oscilloscope, type DuMont 404A. Any piling up showed up very clearly on the oscilloscope picture.

The pile-up limits this experiment in two respects. It proved to be impossible to investigate the high-energy protons from the heavy elements. The gamma-ray and

electron background increases more rapidly with the mass number than does the number of protons. For mass numbers higher than 100, the background was so heavy that it was impossible to operate the counter properly. Another limitation is that most of the gamma rays and electrons are scattered into the forward direction. Therefore it was impossible even for light elements to measure for smaller angles than 45° .

The following four elements were investigated: carbon, aluminum, nickel, and molybdenum. The targets were 25 mm wide and 60 mm long. Values for the target thickness are listed in Table I. The targets were mounted 11 cm from the zinc sulfide screen and followed the rotation of the counter. The plane of the target made an angle of 70° with the axis of the counter.

Figure 5 shows the angular distributions for carbon, aluminum, nickel, and molybdenum. The distributions have been measured several times and the agreement has been within the statistical errors. The experimental points have been fitted with curves of the form $a + b \sin\theta \cos\theta^2$. The values on the constants are listed in Table I. The form of the curves indicates that the forward asymmetry is caused by interference between

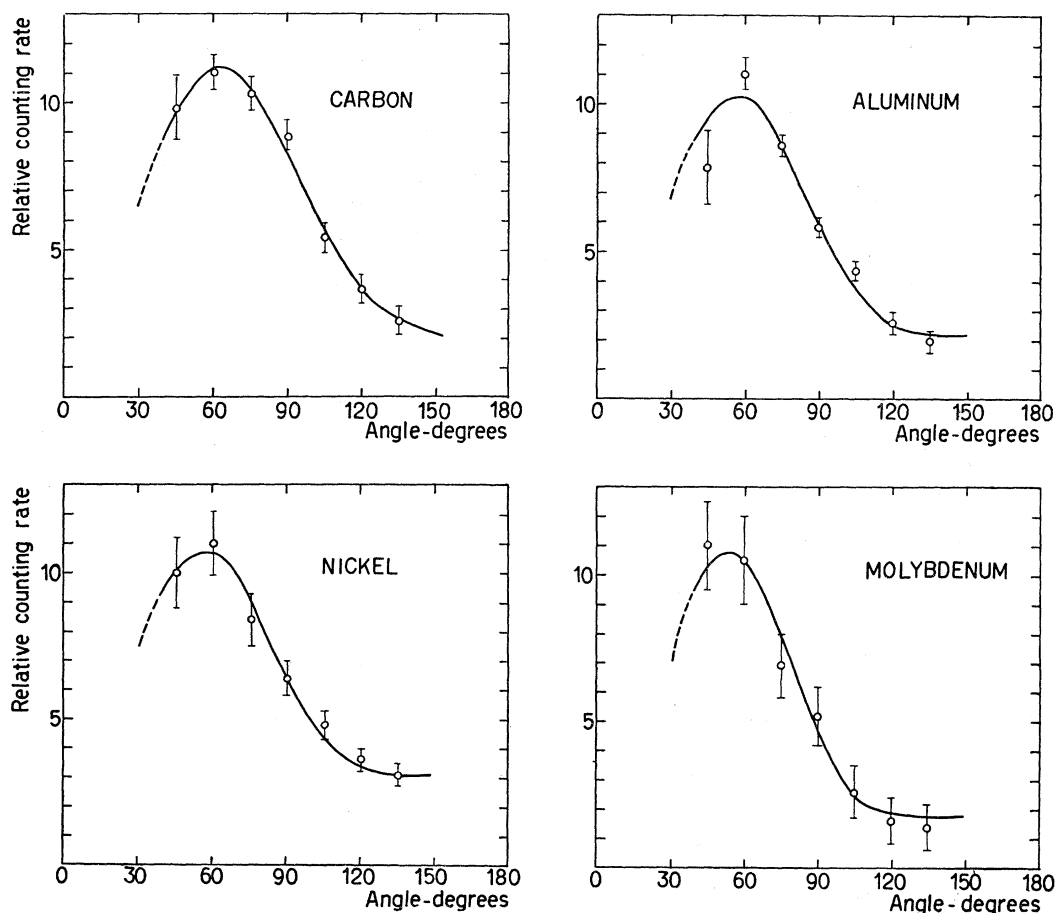


FIG. 5. The angular distributions of protons with an energy above 14 Mev.

TABLE I. Target thickness and the constants a and b in the angular distribution curve $a + (\sin\theta + b \sin\theta \cos\theta)^2$.

Element	Target thickness mg/cm ²	a	b
Carbon	182	0.32	0.80
Aluminum	274	0.58	1.35
Nickel	352	0.94	1.45
Molybdenum	295	0.62	2.00

electric dipole and electric quadrupole photon absorption. The constant b increases with the atomic number, giving an increased forward shift for the heavier nuclei. This means that the quadrupole absorption increases with the atomic number.

It is interesting to compare these results with experiments at other energies. Mann, Halpern, and Rothman⁴ measured the angular distribution of photoprotons using bremsstrahlung of 23-Mev maximum energy. They got curves peaked around 70°. Hendel⁵ used bremsstrahlung of 150-Mev maximum energy and got curves peaked around 50°. Hence the maximum of the angular distribution shifts forward with increasing photon energy.

The constant a is a measure of the isotropic part of the distribution. The isotropic part varies from about 30 percent in carbon to about 50 percent in nickel. One should expect in the direct photoprocess that a certain part of the emitted protons would make collisions with the other nucleons without losing more than a small part of their energy before escaping. Such a process would give an isotropic part in the angular distribution. The nuclei become more transparent with increasing proton energy and therefore the isotropic part should become less. This is actually the case. Angular distributions for 30- and 50-Mev protons⁵ show a considerably smaller isotropic part than the present experiment. It is impossible to decide whether this internal scattering can account for the whole isotropic part. More has to be known about the mechanism of the direct photoemission before this question can be solved. It is interesting to note that the calculations of Courant based on the independent-particle model give a considerable isotropic part. The size of it depends on the quantum state of the emitted nucleon in the nucleus.

Neutrons

The targets in this experiment were blocks of beryllium, aluminum, tantalum, and lead. They were kept in a fixed position. The neutron counter was set in different angular positions around the target. The target-counter distance was 17 cm except for the two smallest and two largest angles, where it was 21 cm. In a separate experiment it was confirmed that the counting rate varied with the inverse square of the distance. The counting rates at distance 21 cm could then be converted to counting rates at 17 cm.

The elastic scattering of the neutrons presents a

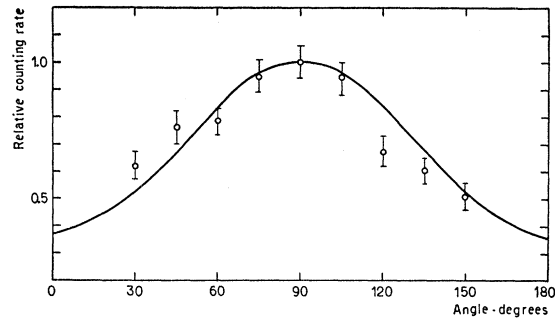


FIG. 6. The angular distribution of the neutrons from beryllium. Counter threshold at 10 Mev.

difficult problem in these experiments. It takes place within the target, in the lead absorber, and also in the material around the counter (lead shield, support). The scattering in the target can be estimated from the size and shape of the target. It turns out to be small. The scattering in the absorber and the surroundings is very difficult to calculate. A very rough estimate shows that it too is small. Because of the complicated nature of the calculations, no attempt has been made quantitatively to correct the measured values for the scattering. It seems certain, however, that it cannot have any essential influence on the results.

The synchrotron was run at constant intensity during this experiment. The intensity was monitored by an ionization chamber as described above. The counter was set at different angular positions and the counting rate was determined. The counting rate without target was then determined under exactly the same conditions and this background was subtracted to get the true counting rate. The background was almost constant for all counter positions (about 20 percent of the counting rate at 90°). The pulse height spectrum falls off very rapidly with increasing pulse height. Therefore the stability of the apparatus is very essential. In order to make sure that the results were not affected by any drift in the electronic circuits the following procedure was followed. The counting rate was first determined at 90°. After a number of readings had been taken in other positions, it was again measured at 90°. If the two counting rates did not agree within the combined standard errors, the whole series was discarded. In most cases, however, the stability proved to be sufficient. The curves were quite reproducible.

Figure 6 shows the angular distribution of the photo-neutrons from beryllium. The threshold of the neutron counter was set at 10 Mev. The experimental points have been fitted with a curve of the form $a + b \sin^2\theta$. The curves for thresholds at 5 and 2.5 Mev are very similar to the one shown in Fig. 6. One might expect them to have a greater isotropic component due to the low-energy evaporation neutrons. The reason that there is no such increase of the isotropic part is probably that

the statistical model does not apply to very light nuclei such as beryllium.

The angular distribution of the aluminum photoneutrons is shown in Fig. 7. The threshold of the neutron counter was set at 2.5, 5, and 10 Mev, respectively. The experimental points have been fitted with curves of the form $a + b \sin^2\theta$. The two curves with thresholds at 5 and 10 Mev are quite similar. The curve for a 2.5-Mev threshold has a much higher isotropic component. The reason is probably that when the threshold is sufficiently low, the evaporation neutrons will be counted, thereby increasing the isotropic part.

Figure 8 shows the angular distribution of the photoneutrons from tantalum. Runs were taken with thresholds both at 5 and at 10 Mev. The experimental points could again be fitted with curves of the form $a + b \sin^2\theta$. The constants are very nearly the same as for the corresponding aluminum curves. The two points at 30° and 45° in the 5-Mev curve deviate considerably from the curve. This is attributed to the scattered gamma rays, which increase the counting rate by piling up. This effect is most likely to occur for heavy elements and in the forward direction. If the threshold is lowered to 2.5 Mev, the whole forward part of the curve is deformed giving a steady increase in counting rate from 150° to 30°.

The angular distribution for the photoneutrons from lead is shown in Fig. 9. The threshold was 5 and 10 Mev. Also in this case the experimental points can be fitted with curves of the form $a + b \sin^2\theta$. The constants have

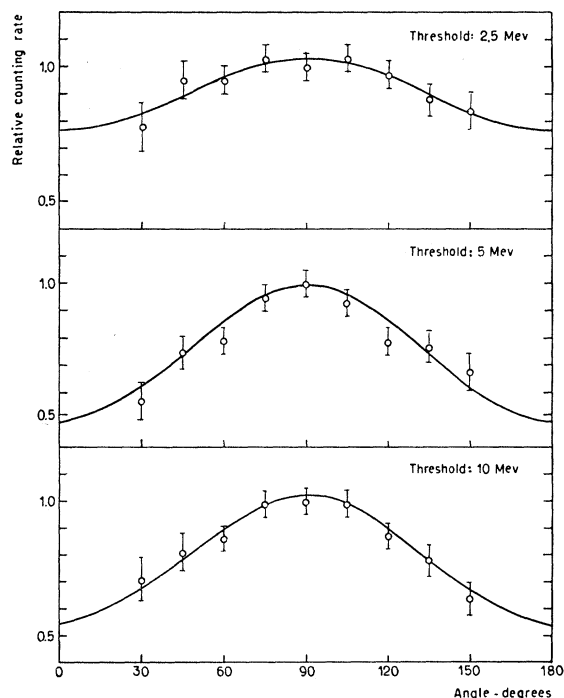


FIG. 7. The angular distributions of the neutrons from aluminum. Counter thresholds at 2.5, 5, and 10 Mev.

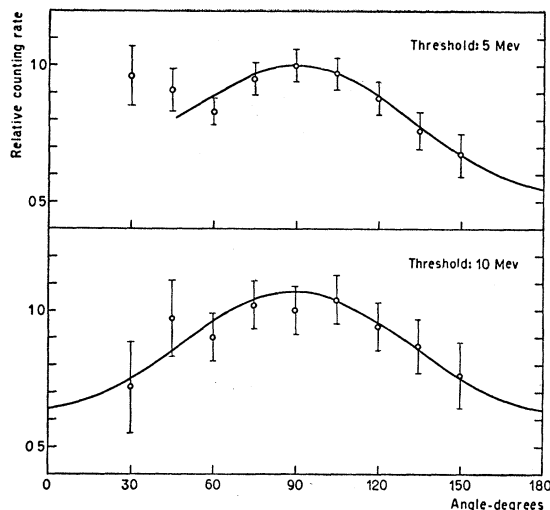


FIG. 8. The angular distributions of the neutrons from tantalum. Counter thresholds at 5 and 10 Mev.

about the same values as for aluminum and tantalum.

The isotropic part has almost the same relative intensity for all the 5- and 10-Mev curves except the one for beryllium. About 60 percent of the neutrons belong to the isotropic component. As discussed above only a small part of it can be attributed to scattering of the neutrons. An effect which might be of greater importance is the lack of an absolutely sharp threshold for the neutron counter. The curves in Fig. 3 have been obtained under very simplified assumptions. It is possible that the sensitivity curve has a tail at the low-energy side, in which case some of the evaporation neutrons might be counted. Even if the sensitivity is very low, the number of evaporation neutrons is so high that it might give a considerable contribution to the isotropic component. If this is true, however, one should expect the isotropic part to be relatively more important with the threshold set at 5 Mev than at 10 Mev. This is not the case. Another indication against this explanation is that Poss,¹⁶ using aluminum as threshold detector, found about the same ratio for the counting rates at 90° and 0° as obtained in the present work. A threshold detector, of course, has a sharp energy cutoff (in the case of aluminum, at 4.6 Mev). Therefore it seems likely that the greater part of the isotropic distribution is real and not due to scattering or instrumental effects.

One might expect a certain fraction of the neutrons to collide with the other nucleons before leaving the nucleus. If the energy loss is small they may still be detected by the counter. This effect gives a contribution to the isotropic component. The same situation for the protons has already been discussed, and the difficulties are the same in this case. A quantitative calculation of the internal scattering is not feasible and therefore it is impossible to know if it can account for the whole isotropic component. It should be noted, however, that in this work the mean energy of the neutrons is lower

than that of the protons. The internal scattering should therefore be of greater importance for the neutrons.

The Yield

Protons

The targets in this experiment were cylindrical with a 44-mm diameter. They were made with varying thickness corresponding to the range of 14-Mev protons in the respective material. The cylindrical plates were mounted in the synchrotron beam so as to make an angle of 15° with the beam. The support was made of plastic film and thin aluminum foil. The counter was set in the 105° position.

The intensity of the synchrotron was kept constant as described above. The maximum bremsstrahlung energy was 65 Mev. The counting rate was determined for each target. The background without target was also determined and subtracted to get the true counting rate. The stability of the apparatus was checked by measuring the counting rate for a copper target several times during the run. The variations were within the statistical errors.

The yield was determined for eight elements: C, Mg, Al, P, S, Ni, Cu, and Mo. The relative yield per mole is plotted against the atomic number Z in Fig. 10. The experimental points fall very well along a straight line. The slope of the line is 0.92. Hence the yield of protons above 14 Mev is approximately proportional to Z .

Neutrons

The neutron yield was determined for 19 elements from carbon to lead. The targets were cylindrical, 44 mm in diameter and of weight 60 grams. They were mounted with the flat side perpendicular to the beam. The support was made of thin aluminum foil and plastic film. The counter was placed 10 cm from the target and in a

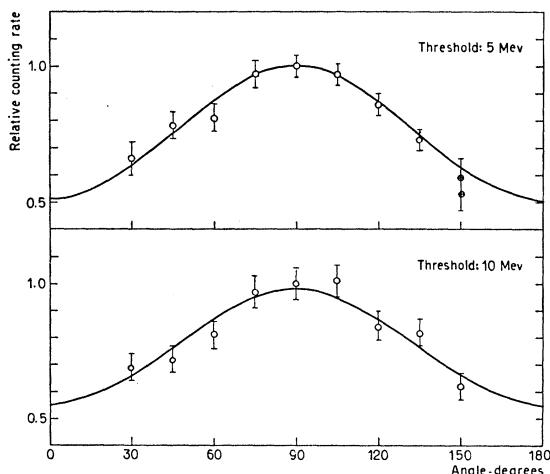


FIG. 9. The angular distributions of the neutrons from lead. Counter thresholds at 5 and 10 Mev.

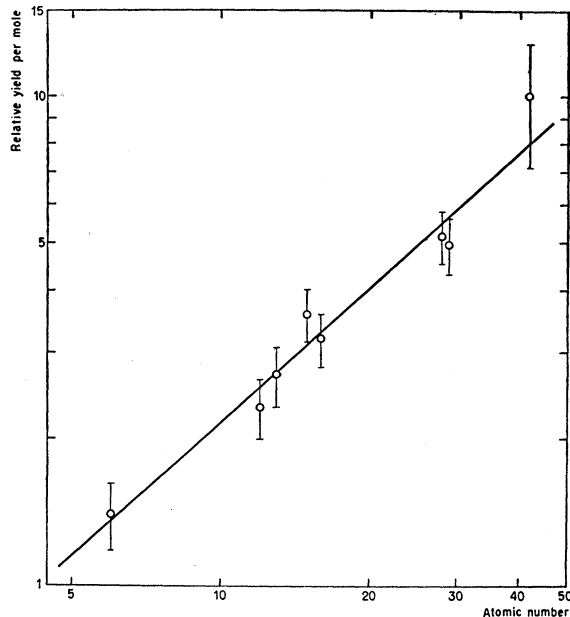


FIG. 10. The relative yield per mole for protons above 14 Mev as a function of the atomic number.

direction making an angle of 105° with the beam. The bremsstrahlung is absorbed to some extent in the target so that the intensity is not constant over the volume of the target. This is especially true for the heavy elements. The thickness of the target was kept so low, however, that this effect was negligible in this experiment.

The threshold of the neutron counter was set at 7.5 Mev. The synchrotron was run at 65 Mev. The experiment was performed in the same way as for the protons. The beam intensity was kept constant and the counting rate determined with and without target. The stability of the apparatus was checked by measuring the counting rate for the aluminum target several times during the run.

The relative yield per mole is plotted in Fig. 11 as a function of the number of neutrons, N . The experimental points fall nicely along a straight line with a slope of 1.05. Hence the yield is nearly proportional to N .

Excitation Curves

The energy distribution of the protons detected by the counter is shown schematically in Fig. 3(c). The greater part of them fall in a fairly narrow range just above the threshold. The distribution is approximately symmetrical with a mean energy of 17.5 Mev and a half-value of 6 Mev. It would be very interesting to know the energy distribution of the photons which cause the emission of these protons. It means that we have to determine the yield of the high-energy protons as a function of the maximum energy of the bremsstrahlung. The dose received by the target was determined by

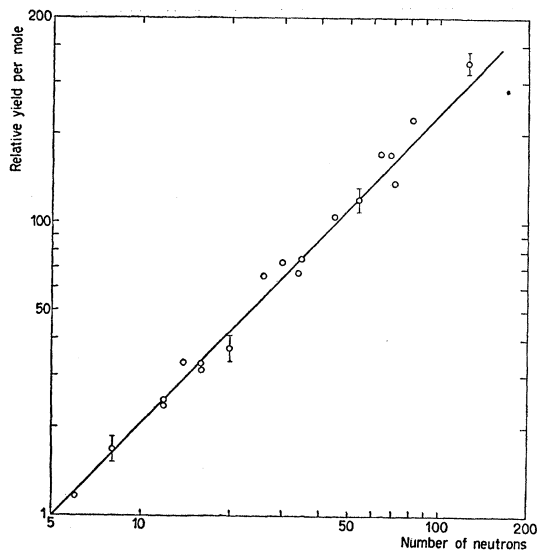


Fig. 11. The relative yield per mole for neutrons above 7.5 Mev as a function of the neutron number.

simultaneous activation of monitor foils. The following procedure was used: The synchrotron was run at a certain energy and with constant intensity. The number of high-energy protons from a thin target was counted for a certain length of time. Foils of zinc or tantalum were activated in the beam during the counting time. The activity of the foils was determined by a thin-walled Geiger-Müller tube under exactly the same conditions every time. Measurements were also made without target to determine the background. The counting rates and activities were determined for a number of different synchrotron energies.

The piling up of electron pulses was a serious limitation in this experiment as well as in all the other proton experiments. The beam intensity was kept very low to make absolutely sure that no pile-up took place. This, of course, made the statistics rather poor, but the results are sufficiently accurate to give the main features of the excitation curves.

Figure 12 shows the excitation curves for aluminum and phosphorus. The ratio between the number of high-energy protons and the activity of the monitor foil is plotted against the synchrotron energy. The monitor foils were in this case made of zinc. The curves are very similar. Starting from about 25 Mev, they rise to about 45 Mev; from there on they are fairly constant. It is rather difficult to make a detailed analysis to find the cross-section curves because of the considerable uncertainty in the activation curves. It is easy to see, however, that the greater part of the cross-section curves falls between 30 and 40 Mev and that they have a maximum around 35 Mev. Hence one can conclude that the protons with a mean energy of 17.5 Mev are mainly produced by photons in the energy range from 30 to 40 Mev.

Coincidence Experiment

For the high-energy photoeffect Levinger²⁰ has proposed a deuteron model. According to this model the photon interacts with a quasi deuteron inside the nucleus. The high-energy protons and neutrons are therefore emitted in pairs. A coincidence experiment was performed in order to see whether the directly emitted protons and neutrons could be produced by a process of this type also at lower energies.

A Lucite target 182 mg/cm² thick was mounted between the proton and neutron counter. The counters were placed in opposite directions at right angles to the beam. They were operated in the way described above. The threshold of the proton counter was 14 Mev as before and the discriminator of the neutron counter was set at 10 Mev. The output pulses from the discriminators were shaped and led to a coincidence circuit. The resolving time was determined from the width of the incoming pulses to be about 0.75 μ sec. The counting rates in the two counters and the number of coincidence pulses were recorded.

With this experimental arrangement a certain number of coincidence pulses was obtained. The neutron counter was then moved 20 cm along the beam so that proton-neutron coincidences no longer should be recorded. Coincidence pulses were still obtained. There was no process which could give rise to true coincidences. Hence all these pulses must be accidental. A calculation using the counting rates, the length of the beam pulses, and the resolving time of the coincidence circuit gave a rate of coincidence pulses in reasonable agreement with the observed one. It was then possible, since the counting rates were known, to calculate the number of accidental coincidences in the first experiment. It turned out that the calculated number of accidental coincidences agreed within the statistical fluctuations with the observed number of coincidences. Hence no true coincidences between protons and neutrons were observed in this experiment.

This does not exclude the possibility that there is a certain number of proton-neutron pairs emitted. However, an upper limit can be set from the information obtained in the experiment. It is then necessary to know the solid angles, the sensitivity of the counters and the angular correlation in the emission of a proton-neutron pair. The solid angles are obtained from the geometry of the experiment and the sensitivities have been calculated. Nothing is known about the angular correlation. Therefore the upper limit for the emission of proton-neutron pairs is calculated for two extreme cases. If it is assumed that the protons and neutrons are emitted in opposite directions the upper limit is 3 percent. If it is assumed that there is no angular correlation the limit is 50 percent. The actual value should be somewhere between these two extreme values. This experiment therefore leads to the conclusion that the number of proton-neutron pairs is less than the number of single protons.

DISCUSSION

The experimental material presented here makes it possible to draw some conclusions about the direct photoeffect. We will compare the experiments with the theoretical calculations of Courant¹⁸ and Levinger.²⁰

Courant's calculations are based on an independent-particle model. The nucleons are assumed to move independently in a square well potential. The cross section for the direct photoeffect is equal to the sum of the cross sections for all the individual nucleons, only dipole photon absorption being taken into account. The angular distribution of the emitted particles is of the form $a + b \sin^2\theta$ for both protons and neutrons. This is exactly the distribution obtained for the high-energy neutrons, but it is in definite disagreement with the experimental angular distributions for the protons. The reason for this disagreement might be that only dipole photon absorption has been taken into account. A calculation²⁶ with electric quadrupole absorption included gives the following results: For neutrons there is no change because the effective charge of a neutron is zero in the quadrupole case. For protons, however, the electric quadrupole absorption gives a forward shift of the peak due to interference. This is in very good agreement with the experimental results.

According to the theory the yield of high-energy protons and neutrons varies roughly as Z^3 . The disagreement with the experiment is perhaps not too serious. The experiment gives the yield of the protons and neutrons above a certain energy. Without knowing the energy distributions one cannot calculate the total yield of the directly emitted particles. A detailed comparison with the theory is, therefore, rather difficult in this case. For the same reason it is impossible to find an absolute value of the cross section for comparison with the theory.

It is easy to calculate approximately the excitation curves for proton production on the basis of an independent-particle model. Assuming a Fermi distribution inside the nucleus we find a mean binding energy of about 18 Mev for aluminum and phosphorus. The protons detected by the counter have a mean energy of 17.5 Mev. We therefore expect the cross section curves to have a maximum at about 35 Mev. This is in very good agreement with the excitation curves in Fig. 12.

The quasi-deuteron model of Levinger is intended to apply to energies above 150 Mev. It would be rather surprising to find it applicable also to the energy range investigated in this work. It might, however, still be of some interest to compare the experimental results with the predictions of the deuteron model. According to this model the angular distributions for protons and neutrons are different because of the interference between electrical dipole and electrical quadrupole terms. In the center-of-mass system the protons are emitted

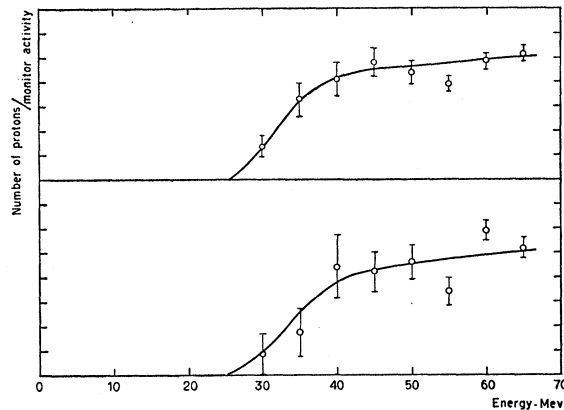


Fig. 12. The ratio between the number of high-energy protons and the activity of the monitor foil as a function of the synchrotron energy. The top curve is for aluminum and the bottom curve is for phosphorus.

predominantly in the forward direction and the neutrons in the backward direction. In the laboratory system the photon momentum shifts both the proton and neutron distributions in the forward direction. The backward shift of the neutron distribution due to the interference is nearly cancelled by the forward shift due to the photon momentum. We therefore have good agreement between the experimental results and the deuteron model in this respect.

According to the deuteron model, the cross section of the direct photoeffect is proportional to NZ/A , or nearly proportional to N and Z . There is good agreement with the experimental results also in this respect, though a literal deuteron model appears to be in very definite disagreement with the experimental excitation curves. One would expect the cross-section curves for the high-energy protons to have a threshold at about 45 Mev and a maximum at about 70 Mev. The excitation curve would then show a steady rise from the threshold at 45 Mev up to about 100 Mev. This is in complete disagreement with the experimental curves.

The coincidence experiment showed that only a rather small number of proton-neutron pairs are emitted. This is also in disagreement with the literal deuteron model. However, the experimental results do not exclude the possibility that proton-neutron pairs are formed inside the nucleus but that for some reason only one of the particles escapes without appreciable energy loss.

The conclusion of this comparison is that the independent-particle model, modified to take quadrupole absorption into account, is in reasonable agreement with the experimental results. The literal deuteron model, on the other hand, agrees with some of the experimental results but is in serious disagreement with others.

The author wishes to thank Dr. D. J. Zaffarano for his invaluable aid during the course of this research. The continued interest and encouragement of Dr. L. J. Laslett is gratefully acknowledged.

²⁶ The author is indebted to Dr. G. Källén for the calculation and for interesting discussions on this subject.